

# The effect of semi-rigid joints on the design of cold-formed steel portal frame structures

R. P. D. Johnston<sup>1</sup>, A. M. Wrzesien<sup>2</sup>, J. B. P. Lim<sup>1</sup>, M. Sonebi<sup>1</sup> and C. G. Armstrong<sup>3</sup>

<sup>1</sup>School of Planning, Architecture and Civil Engineering, Queen's University, Belfast, UK

<sup>2</sup>Department of Civil and Environmental Engineering, University of Strathclyde, Glasgow, UK

<sup>3</sup>School of Mechanical and Aerospace Engineering, Queen's University, Belfast, UK

**Abstract.** This paper investigates the effect of semi-rigid joints and finite connection length on the design of cold-formed steel portal frames. The performance of frames sized using a rigid joint and full joint strength assumption is compared with frames having semi-rigid joints and partial strength. It goes on to describe whether it can offset the fact that the joints cannot sustain the full moment capacity of the sections. Experimental, analytical and finite element modelling techniques have been used. They demonstrate that frames of modest span sized using a rigid joint and full joint strength assumption, are unsafe under gravity load and do not satisfy the ultimate limit state. Designers should therefore take the semi-rigidity and partial strength of the joints into consideration when analysing cold-formed steel portal frames.

## 1 Introduction

Cold-formed steel portal frames can be a viable alternative to conventional hot-rolled steel portal frames for low rise commercial, light industrial and agricultural buildings of modest span (around 10 m) [1-4]. Whilst it is well-known that the eaves and apex joints of such frames possess a reduced moment capacity, compared to that of the channel-sections [5-6] and that the joints are semi-rigid and have a finite connection-length [7], these effects are seldom taken into account by practicing engineers.

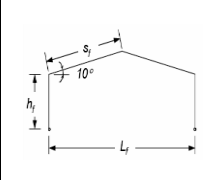
Practising engineers argue that the beneficial effects due to redistribution of forces in the frame and stressed-skin action offset the need to take such joint effects into account in frame analysis. Thus cold-formed steel portal frames in practice, are often designed and analysed on the basis of a rigid joint and full joint strength assumption, with zero connection-length.

Recent research using modern roof panels has demonstrated that stressed-skin diaphragm action, [8-10] can indeed help reduce (or virtually eliminate) frame deflections owing to wind in the horizontal transverse direction for cold-formed steel portal frames [11]. However, for load acting in the vertical / gravity direction (which in the UK would be considered as being snow load), whilst stressed-skin diaphragm action does indeed have an effect when the roof pitch is steep, for flat roofs it has virtually no effect. With the trend of modern roofs becoming flatter, there is therefore the risk that cold-formed steel portal frames in the UK could be unsafe in some cases, under snow load, when sized assuming that stressed-skin diaphragm action takes into account the transverse wind load.

This paper considers the reduction in load carrying capacity of portal frames as a result of the joint effects determined from laboratory tests which were validated against analytical and finite element modelling. Four

frames with following spans and eaves height are considered: 5 m by 3 m, 5 m by 6 m, 10 m by 3m and 10m by 6m. The section sizes were checked under only the vertical / gravity load case, with the joint effects taken into account. The deflection limits and the parameters used for the frames are defined in Table 1.

**Table 1.** Serviceability deflection criteria

	<b>Absolute deflection</b>	<b>Differential deflection relative to adjacent frame</b>
Lateral deflection at eaves	$\leq h_f/100$	$\leq h_f/150$
Vertical deflection at apex	-	$L_f / 200$

## 2 Design Loads

### 2.1 Dead and live loads

The dead and live loads applied to the frame are as follows:

DL due to the self-weight of the cladding = 0.18 kN/m<sup>2</sup>

LL due to snow = 0.60 kN/m<sup>2</sup>

### 2.2 Load Combinations

In accordance with BS5950-1, the frames are sized for the following ULS and SLS load combinations:

ULC1 = 1.4DL + 1.6LL

SLC1 = 1.0DL + 1.0LL (absolute deflection in Table 1)

SLC2 = 1.0LL (differential deflection in Table 1)

### 3 Joint Effects

#### 3.1 Description of joints

Figure 1 details the typical eaves and apex joints. As can be seen, the joints are formed through brackets, bolted to the channel sections used for the column and rafter members.

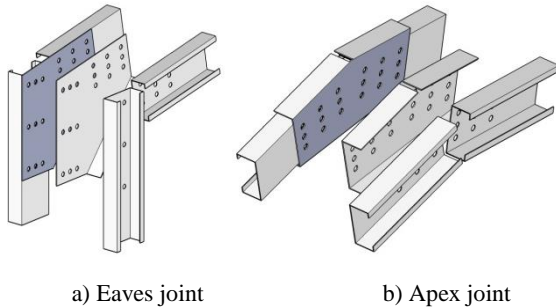


Fig. 1. Bolted Cold-formed portal frame joints

Following industry practise, the connections at the eaves and the apex rafter use a bolt array of the length  $a_B$  equal to the depth of the channel section. All connections use the 3x3 bolt array and M16 Grade 8.8 bolts with fully threaded bolt shank. The length of the bolt-group for the column to the bracket joint was assumed as twice the depth of the channel section.

#### 3.2 Reduced strength of joint

As described by [5-6] if the length of the bolt-group ( $a_B$ ) is short, compared with the depth of the section, the channel-section will fail through premature web buckling. This mode of failure can be taken into account using method presented in [5]. The forces in the member are calculated base on elastic joint design principle and static equilibrium. The channel section is therefore examined based on combine effect of bending and transverse force at the critical cross section. Based on findings presented by [11-12] the strength of each joint is examined based on standard interaction equation between bending and web crippling [13]. It is assumed that members are restrained against lateral-torsional buckling in such frequency, that only local capacity check need to be considered.

$$\text{Member capacity: } F_c/P_{cs} + M/M_c \leq 1 \quad (1)$$

$$\text{Joint capacity: } F_{rb}/P_{bs} \leq 1 \quad (2)$$

$$\text{Joint capacity: } F_w/P_w \leq 1 \text{ where } F_w = V_{IR} \quad (3)$$

$$\text{Joint capacity: } M/M_c \leq 1 \text{ where } M = M_{IR} \quad (4)$$

$$\text{Joint capacity: } F_w/P_w + M/M_c \leq 1.5 \quad (5)$$

$F_c$  = Applied axial load

$P_{cs}$  = Short strut capacity in compression

$M$  = Applied bending moment

$M_c$  = Moment capacity of member

$F_{rb}$  = Resultant force in critical bolt

$P_{bs}$  = Bearing capacity of connected plate

$F_w$  = Concentrated web load

$P_w$  = Concentrated load resistance

$V_{IR}$  = Applied shear force RHS cross section 1

$M_{IR}$  = Applied bending moment RHS cross section 1

#### 3.3 Semi-rigidity of joint

The semi-rigidity of the joints is attributed to bearing of the bolt holes around the bolt shank. From the bolt-hole elongation stiffness, the rotational stiffness of the connection can be determined as described in Figure 2, [14].

$$\delta/F = 15 (10/t_1 + 10/t_2 - 2) 10^{-3} \text{ (mm/kN)} \quad (6)$$

$$k = 3/2 (a_B^2 + b_B^2) F/\delta \quad (7)$$

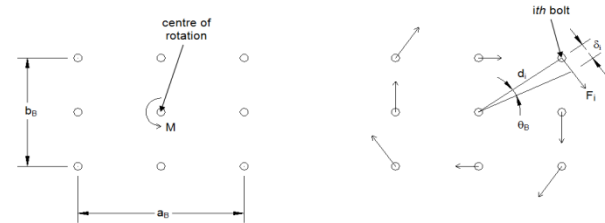


Fig. 2. Rotation of bolt group [14].

### 4 Laboratory Tests

#### 4.1 Back-to-back beam tests

Laboratory tests were carried out to determine the strength and stiffness of three different types of bolt-group arrangements. Tests were conducted on 6 joints, as well as back-to-back continuous members (Figure 3). Each joint test comprised two identical bolt-group arrangements, one on either side of the vertical axis of symmetry. They were tested under four-point bending. For all joint tests, the total length of the test specimen was 3 m and the distance from the end support to the load point is 1 m. To prevent lateral-torsional buckling, lateral restraints were provided at the supports, load points and at the mid-span.

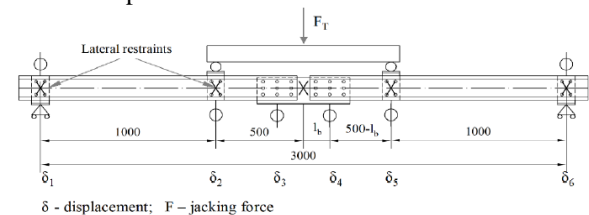


Fig. 3. Laboratory test set-up - back to back beam

Figure 4 demonstrates the various types of failure observed during the laboratory tests on the bending of cold-formed steel sections. Transducers were used to measure the vertical deflection of the bottom flange at the mid-span. Results from the laboratory tests with finite element modelling for the jointed beam considered are presented in Section 6 of this paper.



a) Failure on web                      b) Distortional buckling

**Fig. 4.** Image of laboratory test- back to back beam

### 4.2 Lap joint tests

Single and double cold-formed steel lap tests were carried out, using two transducers to measure displacement through a data logger, which also recorded the tensile load applied. The testing arrangement can be seen in Figure 5a. Stiffened cold-formed sections of 2.0mm, 2.5mm and 3.0mm thicknesses were tested in single and double shear using a fully threaded M16 Grade 8.8 bolt in oversized holes. Four separate tests were carried out for each single and double lap arrangements. Figure 5b demonstrates the typical failure mode of the single lap during the laboratory test.



a) Test set-up                              b) Typical bearing failure

**Fig. 5.** Image of laboratory lap joint test

No torque was applied to the bolt prior to the testing of the lap joint. Within the laboratory tests, displacements were recorded at 0.5kN intervals up to a maximum of 40kN.

## 5 Finite Element Modelling

In order to further check the reliability of stiffness values gained from experimental tests, the experimental results were compared against finite element models for the back-to-back beam and lap joint arrangements. This additional validation meant that the values incorporated within the cold-formed steel portal frame parametric study could be deemed as accurate. The commercial FEA package ABAQUS version 6.11-1 was used to create the geometry, interactions, loading and boundary conditions for both of the laboratory arrangements.

### 5.1 FE - Back-to-back beam test

A static general non-linear analysis was carried out with S4R (reduced integration) shell elements being used to represent the cold-formed steel sections. Figure 6 shows the deflected shape and von Mises stress distribution for the 160mm length jointed beam arrangement.

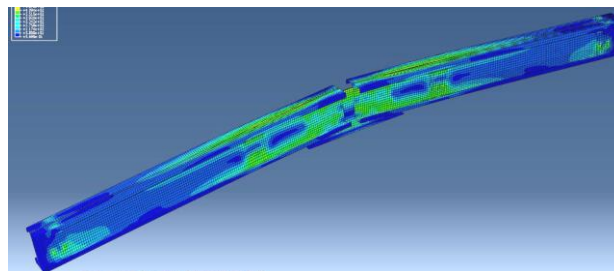


**Fig. 6.** ABAQUS FE shell model of jointed B2B under loading

The bolts were idealised as springs with respective stiffness in x, z and z directions - determined from the laboratory tests described (Section 4.2). Non-perfect geometry was modelled in the analysis – taken from recorded dimensions of the steel samples prior to testing.

### 5.2 FE - Lap Joint test

A static general non-linear analysis was carried out with C3D8R (reduced integration, hourglass control) brick elements used to represent the solid cold-formed steel lap joints and M16 Grade 8.8 bolt. Normal and tangential contacts were used between bolt shank to bolt holes, washer to plate and plate to plate to accurately represent bolt slip, bolt bearing and subsequent tilting. Symmetry was used to reduce computational times, with displacement control loading. Figure 7 and 8 demonstrate the von Mises stress distribution for the FE models under loading.

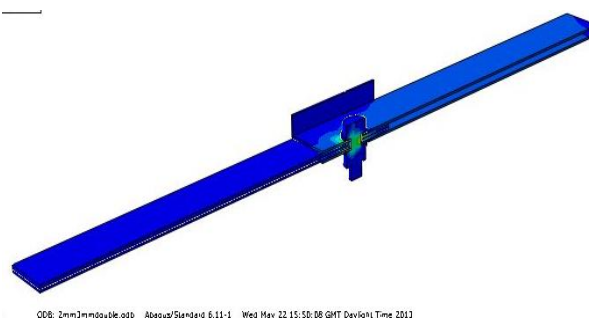


**Fig. 7.** ABAQUS FE solid model of lap joint

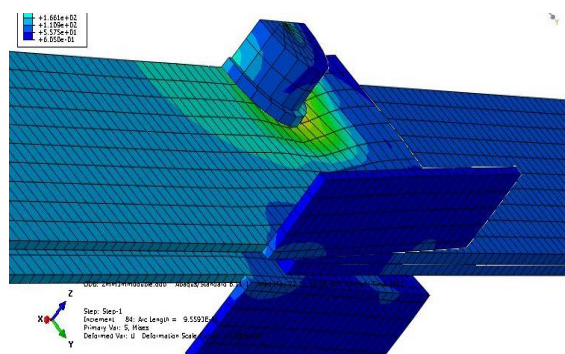


**Fig. 8.** ABAQUS FE solid model of lap joint

## 6 Comparison of laboratory vs FE

### 6.1 Back-to-back beam test

Figure 9 shows the EXP vs. FE comparison for load vs. displacement for both loading cases investigated (jointed beam and continuous beam). The results show close correlation between FE and EXP, with FE marginally stiffer. This can be explained in part due to restraint conditions provided. For the jointed beam, the failure load is observed at 43.34 kN (EXP) and 42.31 kN (FE).

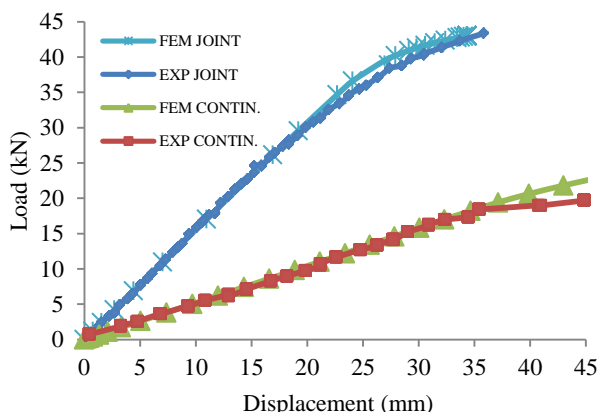


Fig. 9. EXP vs. FE results B2B test

### 6.2 Lap joint test

Figure 10 shows the EXP vs. FE vs. Analytical results for a 2mm/3mm M16 bolt single lap joint test. For clarity, an average EXP result is plotted. The analytical method was taken from [14] equation (6), adding displacement due to bolt slip. Figure 6 demonstrates the good agreement in terms of the stiffness (gradient) over the linear section of the plot, between 4 mm - 6 mm displacement. The graph also shows good correlation between EXP and FE.

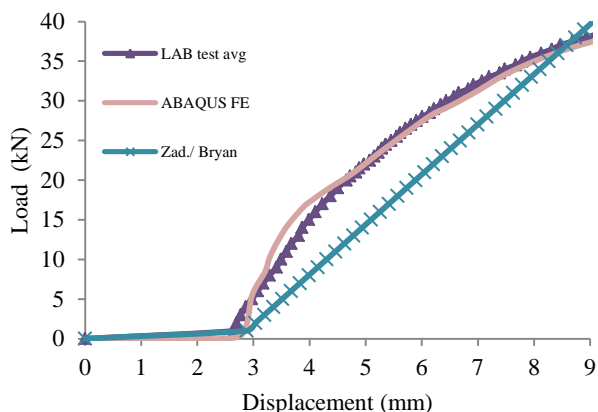


Fig. 10. Lab vs. FE results 2mm/3mm single lap joint test

## 7 Parametric Study

### 7.1 Details of frames

Four frames of modest span were considered, having various dimensions. The following span and height of structure were considered: 5 m x 3 m, 5 m x 6 m, 10 m x 3 m and 10 m x 6 m. The section sizes for the column and rafter members of the frames were designed to satisfy the ultimate and serviceability limit state load combinations.

For each frame, the back-to-back channel-sections used for the column and rafter members of each frame were selected from a database of 20 channel-sections, readily available in the UK. Table 2 shows the back-to-back channel sections used for each frame.

Table 2. Cold-formed steel sections used for column and rafter

Span x Eaves height	Column	Rafter
5 x 3	BBC 15014	BBC 15014
5 x 6	BBC 15016	BBC 15016
10 x 3	BBC 25025	BBC 25025
10 x 6	BBC 25025	BBC 25025

### 7.2 Details of semi-rigidity of joints of partial strength and finite connection length

Table 3 shows details of the rotational stiffness, partial strength and finite connection lengths of the back-to-back channel sections for each connection. The frames were analysed using a beam idealisation, taking into account the rotational stiffness and effective connection length. Figure 11 shows the beam idealisation of the eaves joint. Further details of the beam idealisation model can be found referenced [7].

Table 3. Rotational stiffness of channel sections

Section	Units	BBC15014	BBC15016	BBC25025
$k_{ec}$	kNm/rad	1137	1271	5295
$k_{er}$	kNm/rad	341	381	1779
$k_{ar}$	kNm/rad	341	381	1779
$a_{B,ec} \times b_{B,ec}$	mm	300x80	300x80	500x180
$a_{B,er} \times b_{B,er}$	mm	150x80	150x80	250x180
$a_{B,ar} \times b_{B,ar}$	mm	150x80	150x80	250x180
$l'_{ec}$	mm	121	121	178
$l'_{er}$	mm	196	196	303
$l'_{ar}$	mm	123	123	182

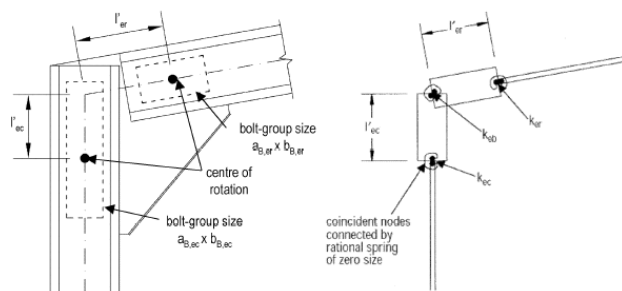


Fig. 11. Beam idealisation of eaves joint

## 8 Results of Parametric Study

### 8.1 Unity Factors

Table 4 shows the unity factors (Applied load/ Capacity) for the frames calculated using a rigid and full joint strength assumption and that with the semi-rigid and partial-strength assumption. As can be seen, the rigid and full joint strength assumption passes both ULS as well as SLS checks. However, when the semi-rigidity and partial strength of the connections are taken into account three out of four frames fail ULS check and all of them fail SLS checks.

Table 4. Unity factors for rigid joint and full joint strength

$L_f \times h_f$	Rigid & full-strength		Semi-rigid & partial strength		ULS <sub>S</sub> /ULS <sub>R</sub>	SLS <sub>S</sub> /SLS <sub>R</sub>
	ULS <sub>R</sub>	SLS <sub>R</sub>	ULS <sub>S</sub>	SLS <sub>S</sub>		
5 x 3	0.92	0.73	1.45	1.28	1.57	1.77
5 x 6	0.88	0.89	1.18	1.52	1.34	1.71
10 x 3	0.97	0.61	0.90	1.05	0.92	1.73
10 x 6	0.89	0.91	1.14	1.45	1.29	1.60

## 9 Conclusion

From results of joint stiffness validation and parametric study, the following conclusions are presented:

1. Frames designed with the assumption of rigid joints and full joint strength to satisfy the gravity load case can potentially be unsafe by as much as 60%. Three out of four frames failed at the apex joint where bending moment has dominant effect.
2. Semi-rigid models presented are valid and have been compared with analytical, experimental and finite element models.
3. Designers should take into account the semi-rigidity and partial strength of the joints in frame analysis.

## References

1. A.H. Baigent, G.L. Hancock, University of Sydney, School of Civil Engineering, Sydney (1978)
2. P. Kirk, *8th International Specialty Conference on Cold-Formed Steel Structures*, St. Louis, Missouri, USA, pp. 295-310, (1986)
3. D. Dubina *et al.*, *4th International Conference on Thin-walled structures*, Loughborough, UK, pp. 381-388, (2004)
4. M. Dundu, A.R. Kemp, *Journal of Constructional Steel Research*, vol. **62**, pp. 250-261, (2006)
5. W.K. Yu *et al.*, *Journal of Constructional Steel Research*, vol. **61**, pp. 1332-1352, (2005)
6. J.B.P. Lim, D.A. Nethercot, *Thin Walled Structures*, vol. **41**, pp. 1019-1039, (2003)
7. J.B.P. Lim, D.A. Nethercot, *The Structural Engineer*, vol. **80**, pp. 31-40, (2002)
8. J.M. Davies, E.R. Bryan, *Manual of stressed skin diaphragm design*. London: Granada, (1982)
9. BS 5950-9, ed London: British Standards Institution, (1994)
10. ECCS, *European recommendations for the application of metal sheeting acting as a diaphragm*. Brussels: European Convention for Constructional Steelwork, (1995)
11. A.M. Wrzesien, J.B.P. Lim, R.M. Lawson, *6th International Conference on Coupled Instabilities in Metal Structures*, Glasgow, pp. 303-310, (2012)
12. D. Dubina *et al.*, *Fifth International Conference on Thin-Walled Structures*. Brisbane, Australia, pp. 387-394, (2008)
13. BS 5950-5, ed London: British Standards Institution, (1998)
14. F. Zadanfarrokh, E.R. Bryan, *11th International Specialty Conference on Cold-Formed Steel Structures*, St. Louis, Missouri, USA, pp. 625-662, (1992)
15. ABAQUS Standard User's Manual, Version 6.11-1 Dassault Systèmes, (2011)